

The Origin of Ice in Mountain Cap Clouds

WILLIAM A. COOPER AND GABOR VALI

University of Wyoming, Laramie 82071

(Manuscript received 29 September 1980, in final form 25 February 1981)

ABSTRACT

Ice crystal development in relatively simple layer clouds was studied using airborne instrumentation. The patterns in the development of ice in those clouds suggest that the ice originates in association with the initial condensation process, near the upwind edge of the cloud. Since continued ice production does not occur beyond that region, the ice development can be attributed to nucleation. There is no evidence for secondary ice generation. Either condensation-freezing or contact nucleation could account for the observed nucleation process, but special properties are required for the nuclei in either case. Ice crystal concentrations show a clear temperature trend, as expected for a nucleation process.

1. Introduction

The results to be presented in this paper are based on observations of the development of ice particles in wintertime clouds of the Wyoming–Colorado region of the Rocky Mountains. These results have emerged from studies we conducted since 1974, and are mostly based on observations obtained using instrumented aircraft. The studies sought to determine the rate of initial ice formation in the clouds and the physical processes involved in that formation.

One motivating force for these studies was that a major share of the precipitation and water supply of the Wyoming–Colorado region, and, indeed, of large parts of the world, involves some form of ice. Another motivation was that basic knowledge about the formation of ice in the atmosphere is still incomplete. While it was recognized at the outset that complete and general answers to the relevant scientific questions would not be produced by a program of relatively restricted scope, it was hoped that some useful deductions would be possible from detailed examinations of the populations of liquid and solid hydrometeors within clouds of relatively simple airflow structure. The study, therefore, emphasized airborne detection of ice crystals and of cloud droplets, and the measurement of other cloud characteristics needed to place the microphysical observations in context. To minimize the need for having to treat in detail the dynamics of the clouds, relatively simple orographic clouds and “cap” clouds (shrouds of clouds enveloping mountain peaks) were studied.

2. Background

The origin of ice elements in clouds, and the correspondence between concentrations of ice particles and of ice nuclei, for several decades have been topics of considerable concern and attention for cloud physicists and for those considering the physics of cloud-seeding with artificial ice nuclei. However, the gradually revealed complexity of the phenomena kept progress slow, so that only partial explanations and incompletely proven hypotheses exist even today.

It is now fairly clearly established that ice elements in clouds have several possible origins, and that the generating mechanisms can be broadly classified as primary or secondary processes. Primary processes are those of nucleation from metastable vapor or liquid: deposition or freezing. Secondary (or multiplication) processes act to increase the concentration of ice particles by interactions involving preexisting ice elements. The known details of these processes are discussed, for example, in Rogers and Vali (1978). Interestingly, existing knowledge about the processes of ice formation in clouds is almost entirely derived from laboratory studies, mostly because of the difficulties of acquiring observations in natural clouds of sufficient acuity and detail to deduce what processes of ice production are at work. Only the operation of two different secondary processes could be confirmed fairly unambiguously in natural clouds: by Mossop (1972) and by Hallett *et al.* (1978) for the rime-splintering process, and by Vardiman (1978), Hobbs and Farber (1972) and Jiusto and Weickmann (1973) for crystal fragmenta-

tion. For primary processes, the only field observation which points to the operation of a particular process is the observation of droplet centers in ice crystals. Auer (1971, 1972) reported observations of drop-centered crystals in natural clouds, and Weickmann (1972) and Parungo and Weickmann (1973) suggested that such crystals originate from frozen cloud droplets. However, this interpretation is not backed by firm evidence, and alternate explanations have been proposed for the presence of spherical particles at the center of crystals (e.g., Katz and Pilie, 1974).

In most studies of natural clouds the principal effort has been to establish the concentration of ice elements which develops as a function of the temperature at the top of the cloud. (The coldest temperature within a cloud was usually assumed to be the most relevant factor, since ice nucleus concentrations increase monotonically with decreasing temperature.) For different types of clouds different patterns are found, revealing the complexity of the problem (cf. Rogers and Vali, 1978). Specifically, studies of ice particle populations in cold stratiform clouds were carried out by only a small number of investigators. Grant¹ reported that in deep clouds over the mountains of northern Colorado crystal concentrations (deduced from the flux of crystals to the surface) correlated with cloud-top temperature, and increased exponentially with decreasing temperature roughly in agreement with ice nucleus measurements. Mossop (1972) and Jayaweera and Ohtake (1973) reported similar, and firmer, results on the basis of observations made from aircraft, also leading to the conclusion that ice crystal concentrations were approximately (to within an order of magnitude) the same as ice nucleus concentrations. On the other hand, Hobbs and Atkinson (1976) reported that even layer-type clouds over the Cascade Mountains of Washington State contained much higher ice crystal concentrations than predicted from ice nucleus data. Thus, once again, the results are not generalizable even for the relatively simple stratiform cloud types. It appears that the situation could be clarified by the identification of the specific processes of ice generation, and of the conditions on which particular processes depend. To make some progress in that direction was the main thrust of the work here reported.

3. Sites of the studies

Most of our studies were in cap clouds over Elk Mountain, Wyoming. Elk Mountain is an isolated

peak of ~ 1.3 km relief which forms the northern end of the Medicine Bow Range. The peak is located at $41^{\circ}38'N$, $106^{\circ}32'W$. An observatory is located near the peak of this mountain so that ground-based observations over extended periods of time could be used to augment the aircraft observations.

Some of the data reported in this paper were obtained over the San Juan Mountain range of south-central Colorado. This range straddles the Continental Divide in the vicinity of $37^{\circ}20'N$, $106^{\circ}30'W$.

4. Aircraft instrumentation

The research aircraft used in these studies was a Beechcraft Queen Air Model B80. It was equipped with sensors coupled to an onboard computer-directed data system. The measured parameters included temperature (two probes, one a reverse-flow probe), pressure, dewpoint (a cooled-mirror device), horizontal wind (obtained from the measurements of a Doppler radar), intensity of turbulence, liquid water content (a Johnson-Williams hot-wire device), airspeed, position (VOR-DME), and Aitken nucleus concentration.

a. Ice crystal measurements

Ice crystal concentrations reported in this paper were obtained in two complementary ways. A continuously recording optical-electronic imaging device recorded particle sizes and shapes continuously, and an ice crystal collector provided spot samples for microscopic examination.

A Particle Measuring Systems² 2D-C probe³ recorded the two-dimensional projected images of particles passing through its sensitive volume, and thus provided a continuous record of ice crystal concentrations, sizes, and shapes. The sampling rate of the 2-D probe at average aircraft speed is $\sim 4 \text{ L s}^{-1}$ for particles of $160 \mu\text{m}$ or larger; for smaller particles there is a gradual decrease in sampling rate with diminishing particle size due to optical depth-of-field reduction. Crystal concentrations down to around 0.01 L^{-1} can be measured with fair reliability. A concentration of 1 L^{-1} observed over a 1 km flight track has a statistical counting error of $\pm 14\%$. The probe has a resolution of $25 \mu\text{m}$. The width of the imaging array is $800 \mu\text{m}$, but this does not preclude the partial imaging of particles of larger sizes. Because of the resolution limit and because of the decreased sampled volume for small particles, the most useful range of the probe is for particles

¹ Grant, L. O., 1968: The role of ice nuclei in the formation of precipitation. *Proc. Int. Conf. Cloud Physics*, Toronto, Roy. Meteor. Soc., 305–310.

² Particle Measuring Systems, Inc., Boulder, CO.

³ Knollenberg, R. G., 1976: Three new instruments for cloud physics measurements. *Preprints Int. Conf. Cloud Physics*, Boulder, Amer. Meteor. Soc., 554–561.



FIG. 1. Photograph of the cap cloud of 18 February 1975. The photograph was taken from a position southwest of Elk Mountain, and the wind was from the left in this view.

$> 50 \mu\text{m}$. Recognition of crystal type is possible for ice crystals $\geq 100 \mu\text{m}$. In the computer processing of the recorded data, artifact images (which can result from liquid water streaming off the leading edges of the light apertures, or from fragments of ice crystals which shatter on the probe tips) were eliminated. With the relatively low liquid water contents of the sampled clouds, artifacts were not a serious problem; only 1–5% of the images were rejected.

For detailed microscopic examination of the ice crystal forms, crystals were captured with the aid of a divergent-flow decelerator tube. Empirical tests, both in a wind tunnel and in flight, have established that the deceleration ratio is 11:1, and have determined that the collection efficiency of the $1.3 \text{ cm} \times 7.5 \text{ cm}$ slide (positioned in the tube at a point 1.7 m from the intake orifice) exceeds 50% for particles $> 30 \mu\text{m}$ and exceeds 90% for particles $> 70 \mu\text{m}$ in diameter. The glass slides, coated with mineral oil and held in a long holder with a sliding shutter, were inserted into the decelerator at the desired times, and the shutter was used to control the exposure of the slide. Exposure times, which were generally chosen according to the concentration of ice crystals indicated by the 2-D probe, varied between 5 and 90 s. The time of exposure was automatically recorded by the data system. Following exposure, the slides were stored in test tubes filled with a silicone fluid (chosen because it did not dissolve the mineral oil coating on the slides) and the test tubes were preserved in dry ice. Tests have shown that there was

no appreciable degradation of the crystals over tens of hours, and that only in rare cases (with large three-dimensional crystals, such as complex side-plane structures) was there any appreciable loss of crystals from the surface of the slide. Slides were examined under hexane and photographed at about $10\times$ magnification, usually within $\sim 6 \text{ h}$ after each flight. Excellent image quality was obtained in this manner, so that crystal habit, size and degree of riming could be determined. This was the main utility of the technique, but concentrations were also determined from some of the slides to provide a check on the 2-D probe data.

Detailed comparisons have shown that ice crystal concentrations determined by the two independent techniques are in excellent agreement; for example, for crystal sizes larger than $50 \mu\text{m}$, a set of 12 comparisons (discussed in Cooper and Saunders, 1980) yielded the ratio (2-D:slide) of 1.7 ± 0.9 . Size determinations of crystals are accurate to $\pm 25 \mu\text{m}$ for 2-D data and $\pm 10 \mu\text{m}$ for slide collections.

b. Cloud droplet measurements

Droplet size distributions were measured continuously by a light-scattering device manufactured by Particle Measuring Systems (Model ASSP). This device measures the number and size of droplets passing through its sensitive volume; 15 size intervals of either 1 or $2 \mu\text{m}$ in width were used. The sampling rate of the probe at typical aircraft speeds was $\sim 50 \text{ cm}^3 \text{ s}^{-1}$. Sizing accuracy of the instrument

was checked by calibrations with size-sorted glass beads; these tests indicated probable sizing errors approximately equal to the bin widths. In poly-dispersed clouds the size spectra were found to be broadened by the instrument to greater degrees than indicated by the bead calibrations.⁴ Concentration determinations were subject to error due to limitations of the techniques used for determining the laser beam diameter and the optical depth of field of the instrument, and due to non-ideal behavior of the velocity rejection circuitry employed in the device; we estimate the droplet concentrations to be accurate to within $\pm 30\%$. In addition, the existence of a systematic error in the droplet counts was later discovered: an electronic dead-time in the instrument led to coincidence losses of $\sim 30\%$ for concentrations $\sim 400 \text{ cm}^{-3}$ and of $\sim 50\%$ for concentrations $\sim 1000 \text{ cm}^{-3}$. For concentrations exceeding 1000 cm^{-3} , no reliable corrections could be made for this undercounting due to a saturation effect. Concentrations in these wintertime clouds were below this limit, and the data presented in this paper have been corrected for coincidence losses.

An impactor device using soot-coated slides was also used to determine the cloud droplet distribution at selected locations, and a Johnson-Williams hot-wire instrument provided an alternate measurement of liquid water content.

5. Case studies

a. 18 February 1975

The 18 February 1975 cloud (shown in Fig. 1) was a fairly typical Elk Mountain cap cloud. A cold front had moved through the region of Elk Mountain the day before, and light snow had fallen on the mountain and on the valley to the west of the mountain. When the cap cloud formed, the wind was westerly at $10\text{--}15 \text{ m s}^{-1}$. The sounding (Fig. 2) shows a pronounced inversion near the mountaintop and shows

⁴ Walsh, P. A., 1977: Cloud droplet measurements in wintertime clouds. M.S. thesis, University of Wyoming, 170 pp.

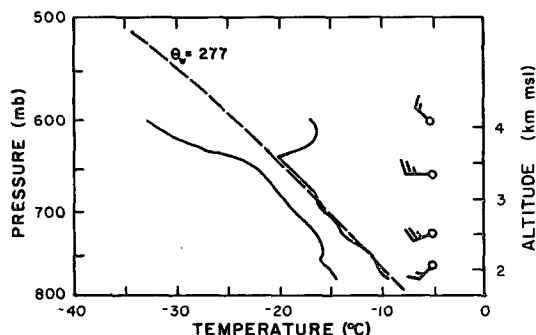


FIG. 2. Sounding of temperature, dew point and wind measured $\sim 25 \text{ km}$ west of Elk Mountain on 18 February 1975. A line of constant wet-bulb potential temperature is shown for reference. Full wind barbs represent 5 m s^{-1} .

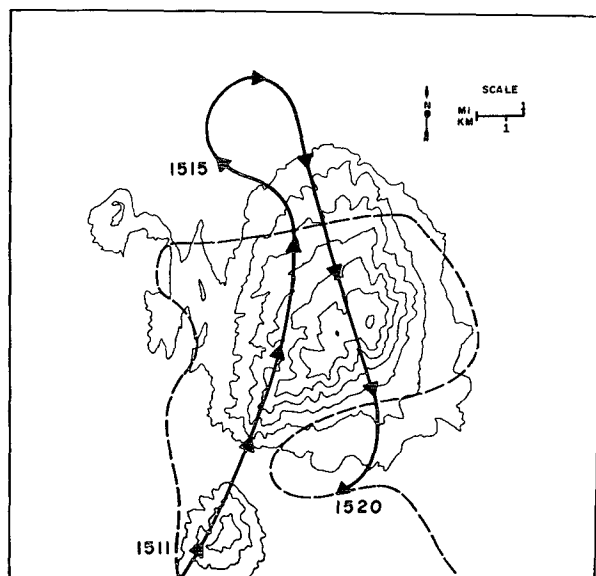


FIG. 3. A typical flight segment penetrating the cap cloud of 18 February 1975. The dashed line shows the approximate maximum horizontal extent of the cloud. The heavy solid line with arrows indicates the flight track (with times shown in local times). The summit is at 3400 m msl , and the contour interval is 150 m . There are other peaks of similar elevation to the south of the region shown in this figure.

the winds to veer with altitude, both usual features of cap cloud situations. The layer in which the cloud formed had an almost constant value of the wet-bulb potential temperature, and the cloud that formed exhibited a laminar structure with no evidence of convection.

Fig. 3 shows the topography of the mountain, the cloud outline, and the path of a typical aircraft penetration through this cloud. The cloud-top altitude was $\sim 3.7 \text{ km msl}$ and the cloud base was near 3.0 km msl . The temperature was -18 to -20°C through the cloud. Seven penetrations similar to that shown in Fig. 4 were made through this cloud.

Fig. 4 shows the temperature, dew point, ice crystal concentration, liquid water content (determined by the ASSP) and horizontal wind measured during the northbound leg of the flight segment shown in Fig. 3. There was strong diffidence around the mountain and confluence through the pass to the south of the mountain. The ice crystal concentration was relatively uniform through most of the cloud, and the ice cloud extended beyond the sides of the water cloud. The liquid water content was quite low, but the peak value agreed with the value expected at a point $\sim 200 \text{ m}$ above the cloud base. The water content due to the ice was still negligible at this point in the cloud.

Fig. 5 is a similar plot for the parameters measured during the pass over the summit, during the southbound leg of the flight segment shown in Fig. 3. The constant altitude aircraft path penetrated the

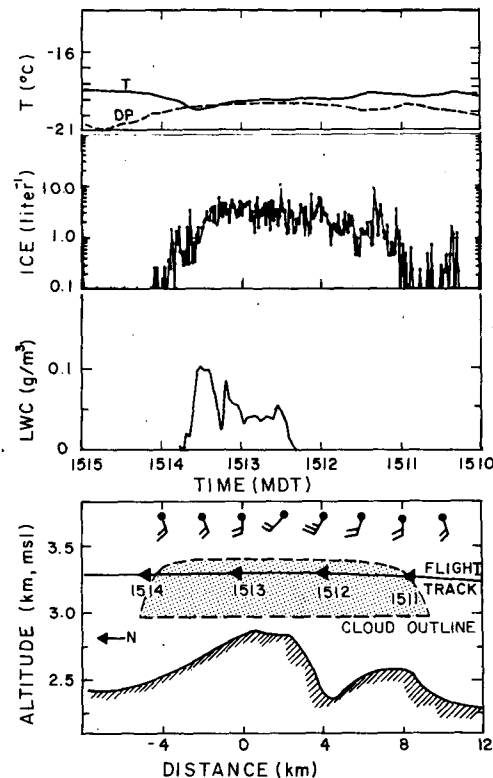


FIG. 4. Top: Temperature and dew point, ice crystal concentration, and liquid water content during the northbound leg of the flight segment shown in Fig. 3. Bottom: The profile of the terrain over which the aircraft flew, the approximate cloud outline, and the winds during the same cloud penetration. This is a vertical cross section plotted as it would appear when looking toward the east (or downwind). The winds are plotted with north to the left, and east upward; full wind barbs represent 5 m s^{-1} .

inversion over the summit, showing the inversion to be pushed upward over the mountain. The ice crystal concentration in Fig. 5 is relatively uniform and does not seem to be correlated with fluctuations in the liquid water content. Both the ice and water portions of the cloud were sharply bounded by the inversion. No ice crystals were detected above the inversion, and no cirrus clouds were present.

Fig. 6 shows the path of a later penetration. A very low concentration of ice crystals ($<0.05 \text{ L}^{-1}$) was found upwind of the visible cloud. About 1 km downwind of the visual or liquid water cloud edge, however, a significant increase in ice crystal concentration was detected. At point A in Fig. 6, the ice crystals were $\sim 100 \mu\text{m}$ in diameter, a size consistent with an origin very near the upwind edge of the cloud. The 2-D images at point A are shown in Fig. 7a. The ice crystal concentration at this point was $\sim 4 \text{ L}^{-1}$. At point B, slightly deeper into the cloud, the crystal concentration was $\sim 6 \text{ L}^{-1}$, and the mean crystal size had increased to $\sim 150 \mu\text{m}$; sample 2-D images from point B, are shown in Fig. 7b. At point C, the crystal concentration was $\sim 8 \text{ L}^{-1}$, and the typical crystal

size was $\sim 200 \mu\text{m}$, as shown in the 2-D images of Fig. 7c. Finally, during the pass over the summit at point D, the crystal concentration was measured to be $\sim 8 \text{ L}^{-1}$ and the mean crystal size was $\sim 300 \mu\text{m}$, as shown in Fig. 7d.

The uniformity in ice crystal concentrations suggests that most of the ice formed within $\sim 1\text{--}2 \text{ km}$ of the upwind edge of the cloud. In the region upwind of the cloud edge, an ice crystal concentration of only about 0.05 L^{-1} was measured, a concentration similar to the concentration of crystal images $> 250 \mu\text{m}$ in Fig. 7a. Within $1\text{--}2 \text{ km}$ downwind of the cloud edge, however, a concentration of 8 L^{-1} had developed. There was no indication of a further increase in that ice crystal concentration as the air moved deeper into the cloud.

The same conclusion is suggested by comparison of Figs. 4 and 5: the ice crystal concentrations were almost the same during these two cloud passes, although one was within $\sim 2 \text{ km}$ of the upwind edge of the cloud and the other was over the summit.

Further evidence that the ice originated near the cloud edge comes from size spectra of the ice crystals. Fig. 8 shows the spectra measured at points A, B, C and D of Fig. 6. The mean size increases with

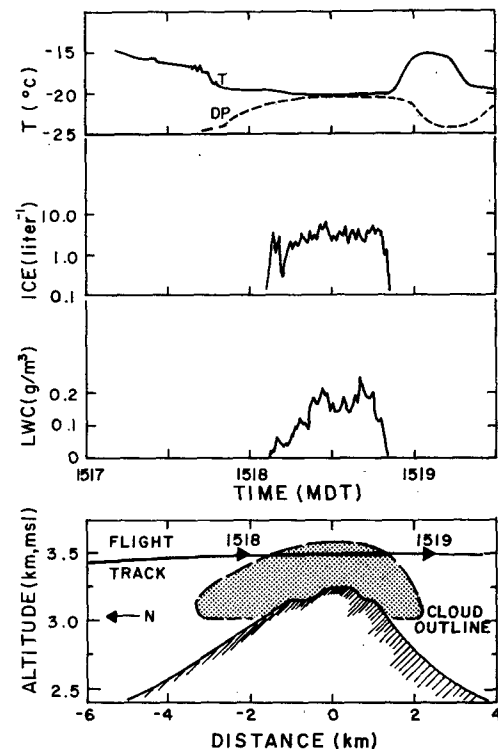


FIG. 5. Top: Temperature and dew point, ice crystal concentration, and liquid water content measured during the southbound flight segment shown in Fig. 3. Bottom: The profile of the terrain over which the aircraft flew, and the approximate cloud outline, during the cloud penetration. This figure is a vertical cross section plotted as it would appear when looking toward the east (or downwind).

distance into the cloud, and at point D there are few ice crystals smaller than $100\text{ }\mu\text{m}$. Furthermore, the size of the crystals at D ($300\text{--}400\text{ }\mu\text{m}$) correlates well with an estimated growth time from the leading edge of the cloud of $400\text{--}600\text{ s}$. Since the ice crystal growth rate is almost a linear function of time (Ryan *et al.*, 1976), a constant production rate would result in a uniform size spectrum. The nonuniform nature of the size distribution in Fig. 8d indicates that the production of ice crystals also is nonuniform in time.

Fig. 9 shows representative ice crystal concentrations measured during the total of seven passes at various points in the cloud. Although there is some variation in the ice crystal concentration, there is no indication that the concentration increases significantly beyond a $1\text{--}2\text{ km}$ region near the upwind edge of the cloud.

Fig. 10 shows some of the ice crystals collected on glass slides. The crystals in the upper left of this figure were collected at points deeper in the cloud. It is interesting that most of the crystals were double-plane crystals, with an apparent droplet at the center. The suggested explanation (Weickmann, 1972) that such crystals originated from frozen droplets is consistent with our observation that most of the crystals appeared after a liquid cloud had formed.

b. 10 January 1975

An example of a cap cloud at cold temperatures (-24 to -27°C) occurred on 10 January 1975. This followed the passage of a cold front during the previous day when the Elk Mountain Observatory was

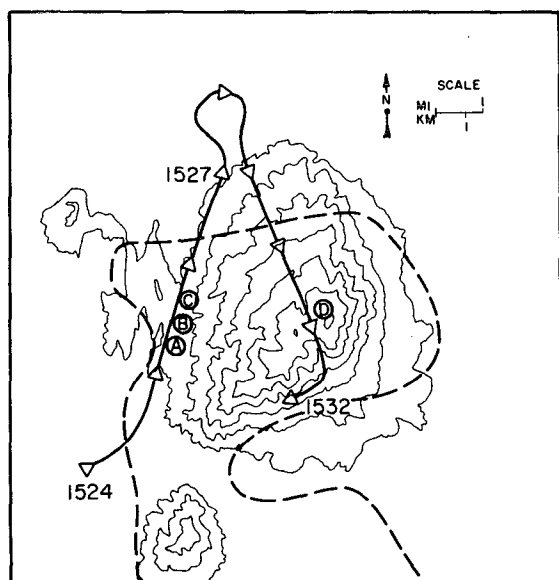


FIG. 6. Another flight segment, similar to that shown in Fig. 3. The locations denoted by letters are discussed in the text.

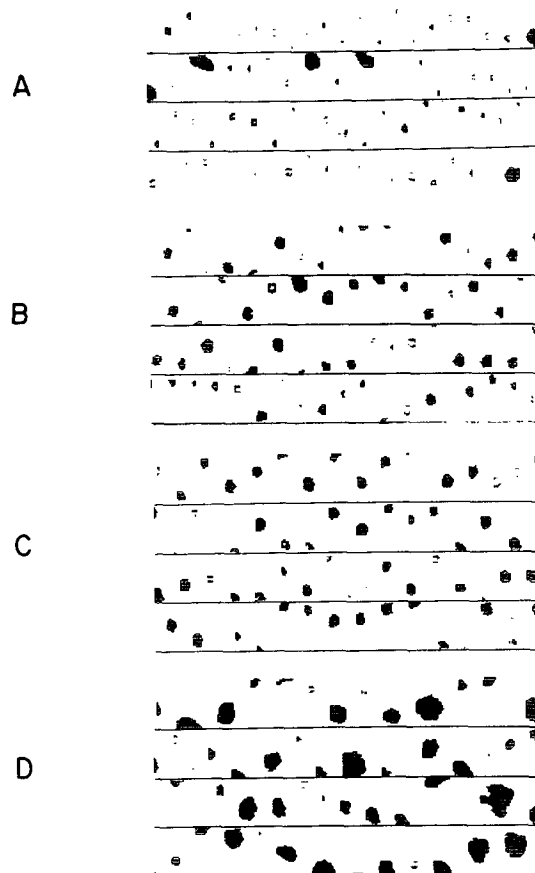


FIG. 7. Representative 2-D images recorded during the flight segment shown in Fig. 6. The horizontal strips show sequences of two-dimensional images of ice crystals that entered the probe aperture. The letters A–D correspond to the locations shown in Fig. 6. The distance between horizontal lines corresponds to $800\text{ }\mu\text{m}$, and the probe resolution is $25\text{ }\mu\text{m}$.

in cloud intermittently and light snow fell. At temperatures around -16°C the concentration of the ice crystals, in cloud, was around 10 L^{-1} . During the night and through the morning of the 10th, the observatory was in a dense cloud. The lowest temperature reached was -26°C and by mid-morning the temperature rose to -23°C .

Some thin cirrus at $\sim 8\text{ km}$ covered most of the area in the morning, but the thickness and areal extent of the cirrus gradually diminished with time. Stratus at $\sim 3.5\text{ km}$ altitude was fairly widespread to the north and south of Elk Mountain. The layer of air below the cirrus was stable with a 4°C inversion at 4 km ; the dew-point depression was $<5^\circ\text{C}$ at all heights. Winds were from the west.

At the time of the research flight, the cloud over Elk Mountain had a well-defined upwind boundary and was a relatively thin layer ($\sim 600\text{ m}$) extending to the south over the entire Medicine Bow range and merging with the stratus to the north. On the east side the cloud swept down close to the mountain

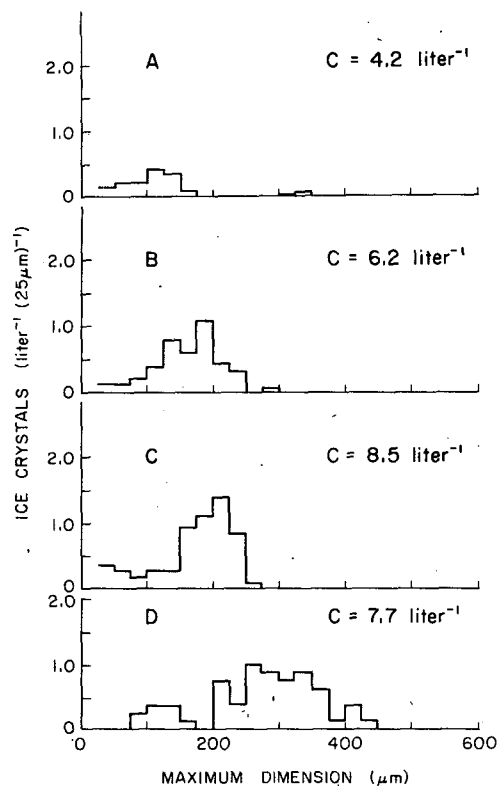


FIG. 8. Ice crystal size distributions, determined from 2-D records, for points A–D shown in Fig. 6.

surface, new clouds formed in the hydraulic jump zone 5–10 km further downwind, and wave clouds formed at ~ 6 km altitude. A photograph of the cap cloud is shown in Fig. 11.

Aircraft sampling of this cloud was performed over the period 1045–1145. Passes were made in the clear air over the cap cloud and through the top of the cloud, four penetrations were made into the leading edge of the cloud, and four oval tracks were flown downwind of the mountain.

The flight segments over and upwind of the cap cloud revealed the sporadic presence of large ice crystals of up to $1500 \mu\text{m}$ size in concentrations around 0.2 L^{-1} . One short period with 0.6 L^{-1} was also observed. The origin of these crystals is uncertain: they either fell from the Ci layer or formed in ice-supersaturated air at lower levels. The crystals were of complex shapes not readily assignable to specific growth regimes.

All four penetrations into the leading portions of the cloud showed a consistent pattern: numerous small crystals were present in rapidly increasing numbers with increasing distance into the cloud. To illustrate this observation, Fig. 12 shows the relevant data from pass 5 at 1117 MST in fact, this example is representative of all four passes. Fig. 12a shows the flight track and the cloud outline with respect to the 2400 m contour line and the position

of the Elk Mountain Observatory (EMO). The region of greatest liquid water content is also indicated (by the inner arc of wavy line); this region seems to line up with the spine of the mountain along the mean wind direction. Horizontal diffuence was evident in the Doppler-observed wind vectors, as indicated. The leading edge of the cloud was further upwind from the mountain on the south side than on the north side. The maximum sustained liquid water content along the flight track was $\sim 0.2 \text{ g m}^{-3}$. Droplet concentrations (N) were highest in the region of maximum liquid water content, pointing to maximum updrafts for that region. The cloud droplet spectrum there had a mode of $8.4 \mu\text{m}$ diameter and a standard deviation of $3.2 \mu\text{m}$.

The histogram in Fig. 12 depicts the particle concentrations measured with the 2-D probe during Pass 5. Fig. 13 shows, as an example, 2-D images from a portion of this pass, demonstrating the presence of a small number of large crystals ($>400 \mu\text{m}$) and many small ones ($<200 \mu\text{m}$).

Since comparison of 2-D data with slide collection is most appropriate for crystals $> 50 \mu\text{m}$, shading has been added to Fig. 12 under the histogram to indicate the 2-D concentration of particles $> 50 \mu\text{m}$. The long rectangle labeled OH-2 shows the average concentration derived from the slide collection made over the indicated period.

The growth habits of the crystals were established from the slide collection. The predominant crystal type was the hollow column, or Clf type, as shown in Fig. 14. These crystals were all $<150 \mu\text{m}$ long. The columnar crystal habit is what would be expected to grow at -23°C and water-saturated con-

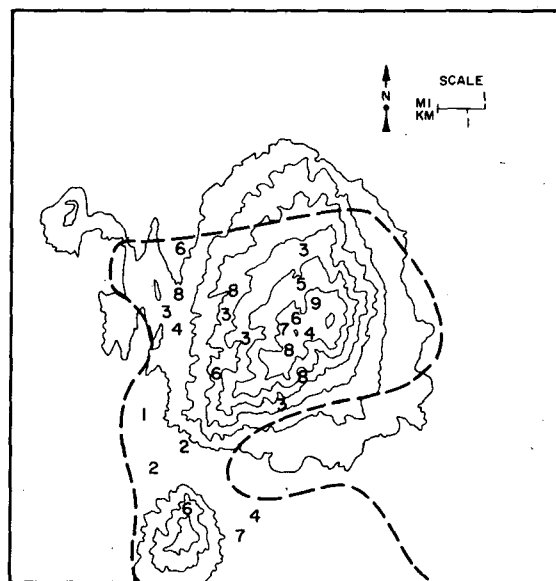


FIG. 9. The cloud outline and contour map as shown in Fig. 3. The superimposed numbers represent ice crystal concentrations measured at various locations within the cap cloud (L^{-1}).

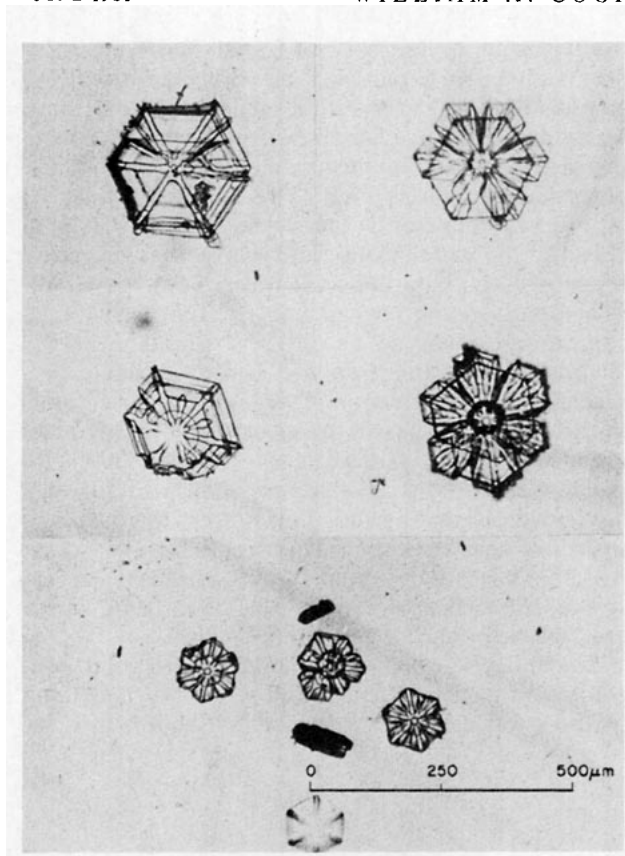


FIG. 10. Examples of ice crystals collected on oil-coated slides exposed in the decelerator during the 18 February 1975 flight. The crystals at the bottom were collected near point C in Fig. 6, and the other crystals were collected at locations further downwind.

ditions (Kobayashi, 1961; Rottner and Vali, 1974). The rare large crystals on the slides were of the complex plate and side plane types. These can be associated both in size and in concentration with the crystals which existed outside the liquid water cloud, but they present a puzzle. Their crystal habit is indicative of growth at temperatures warmer than -20°C and at supersaturation with respect to water, but no such conditions existed upwind of the cap cloud.

At the time of the flight, the observatory temperature was -23°C , the same as at the level of aircraft penetrations in the leading edge of the cloud. Ice crystal samples were frequently taken: the total concentration of crystals was 900 L^{-1} in the mean and varied by about $\pm 30\%$ with a time scale of ~ 30 min. The size distribution of the crystals was distinctly bimodal. About 90% of the crystals were columns (Clf) of $<150\text{ }\mu\text{m}$ length and $\sim 10\%$ were larger columns (Clf) $>250\text{ }\mu\text{m}$ long. In addition, there were occasional complex platelike crystals of $>500\text{ }\mu\text{m}$ size. The largest crystals clearly correspond to the crystals which were present in the air prior to liquid cloud formation. The large columnar crystals correspond in number and in size (after additional growth) to the crystals observed by the aircraft near the leading edge of the cloud. The many small columnar crystals evidently originated near the mountain surface; their sizes are compatible with origins within the cloud-covered portion of the mountain upwind of the observatory.

Based on the aircraft observations over the first



FIG. 11. Photograph of the cap cloud of 10 January 1975. The view is toward the east. Above the cap cloud thin patches of cirrus and wave clouds are visible. The horizontal angle of view is 65° .

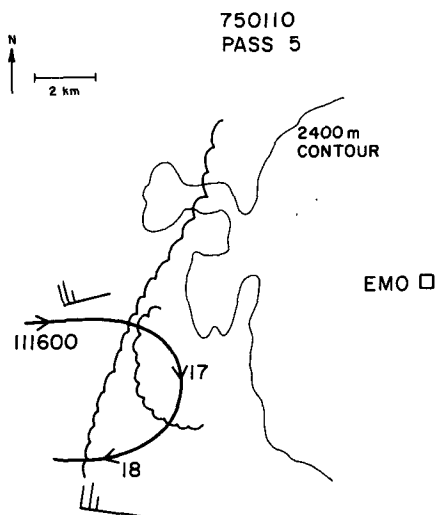


FIG. 12a. The location of pass 5 through the cap cloud of 10 January 1975.

four kilometers of the cloud, and on the measurements taken at the observatory, the approximate rate of crystal formation was deduced. In Fig. 15

the trend in the increase of ice crystal concentration is given for a parcel of air as a function of the elapsed time after formation of liquid water cloud. Times given in Fig. 15 are based on the distance from the observation points to the cloud edge and on the observed horizontal wind. The horizontal line (A) in Fig. 15 represents the crystals which existed ahead of the water cloud, and whose concentration remains essentially constant throughout the cloud. The rapidly rising curved line (B) represents concentrations observed at different points near the leading edge of the cloud. The solid triangle represents the concentration of large columnar crystals at the observatory; this point confirms the plateau in curve B. The rise-time of curve B is ~ 200 s, so that concentrations change less than a factor of 2 beyond about that period. This pattern is consistent with that described for the 18 February 1975 case. All other cases we studied showed similar patterns, so that this behavior can be concluded to be a general characteristic of cap clouds.

The full circle in Fig. 15 depicts the total concentration of crystals at the observatory, but most of these crystals were only $100\text{--}200\text{ }\mu\text{m}$ in size,

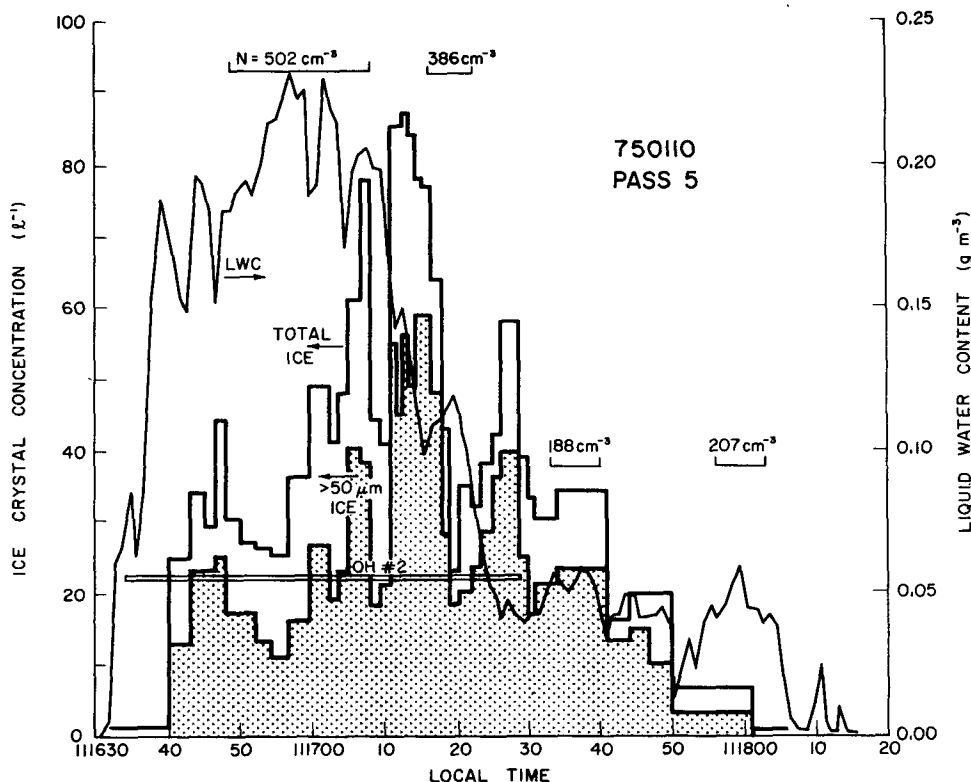


FIG. 12b. Summary of cloud droplet and ice crystal data for Pass 5 in the leading edge. The temperature at the flight altitude was about -23°C , and at cloud base about -19°C . The shaded histogram shows the concentration of ice crystals $> 50\text{ }\mu\text{m}$, and the histogram labeled "total ice" shows the total concentration detected by the 2-D probe. For comparison, the concentration determined from an oil-coated slide also is shown (as the line labeled OH #2) over the interval for which it was exposed. The liquid water content (LWC) was determined by an ASSP, and some representative droplet concentrations are also shown. Full wind barbs represent 5 m s^{-1} .

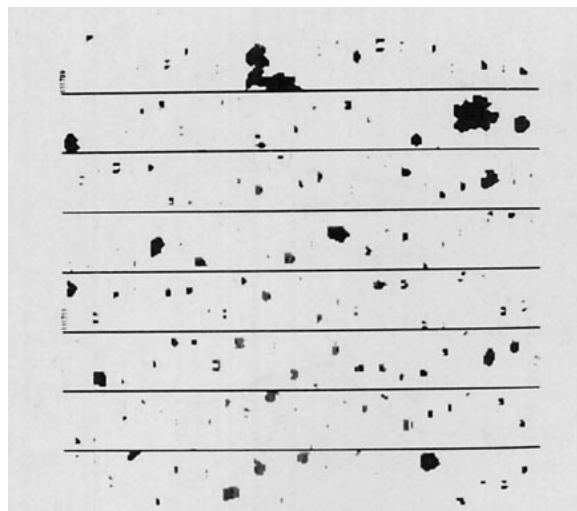


FIG. 13. Examples of the 2-D images recorded during pass 5 on 10 January 1975.

indicative of an origin close to the observatory. This phenomenon of crystal production near the mountain surface was discussed in some detail by Rogers.⁵

During a very shallow penetration into the cloud (<100 m below cloud top) over the observatory still only the sparse concentration ($\sim 0.2 \text{ L}^{-1}$) of large crystals were detected. In comparison to other portions of the cloud, the cloud top appeared to have an ice-free zone relative to the main body of the cloud, probably due to sedimentation of the crystals relative to the air. The temperature at cloud top was -27°C at the highest point of the cap cloud dome, representing about a 3°C cooling in comparison to the cloud top over the leading edge of the cloud. Evidently, this much additional cooling does not create appreciable concentrations of new ice crystals beyond those forming close to the leading edge. It also is evident from this aircraft penetration that the high ice-crystal concentration generated at the mountain's surface does not prevade the entire cloud depth, due to the thermodynamic stability of the cloud. Some mixing with cloud-free air at the cloud top is indicated by a factor of 3 drop in cloud droplet concentration in comparison to the concentration observed in the upwind portion of the cloud. Apparently no new ice crystals originated in association with this mixing process, at least not in sizes and concentrations which could be detected by the airborne systems.

c. 29 December 1974

A deep orographic cloud was studied over the San Juan Mountains of southwestern Colorado on

⁵ Rogers, D. C., 1976: A comparison of surface and airborne ice crystal observations in orographic clouds. *Preprints Int. Conf. Cloud Physics*, Boulder, Amer. Meteor. Soc., 468–471.

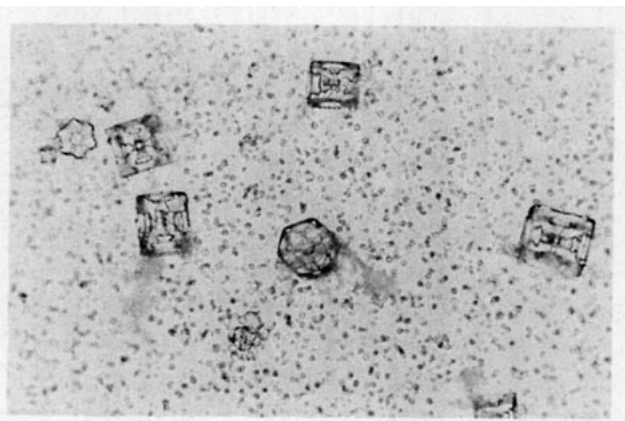


FIG. 14. Samples of the ice crystals collected during pass 5 on 10 January 1975. The largest crystal in this set is $120 \mu\text{m}$ long. The smaller objects are cloud droplets.

29 December 1974, during the Colorado River Basin Pilot Project. The leading edge of this cloud was well defined and the airflow into that edge was smooth, so that this cloud also provided an opportunity to study the development of ice within the cloud. Fig. 16, adapted from Fig. 7 of Cooper and Saunders (1980), shows the outline of the cloud and the flight track for this case study. Flight above the cloud verified that no crystals were falling into the cloud from high levels; the top of the cloud was capped by an inversion and a dry layer with 10°C dewpoint depressions. Other aspects of this cloud have been discussed in Cooper and Saunders (1980).

The concentrations of ice crystals in the cloud are indicated in Fig. 16 by contour-lines which are based on measurements taken at three different flight levels. The colder upper regions of the cloud developed higher crystal concentrations than the lower, warmer regions, although this difference becomes some-

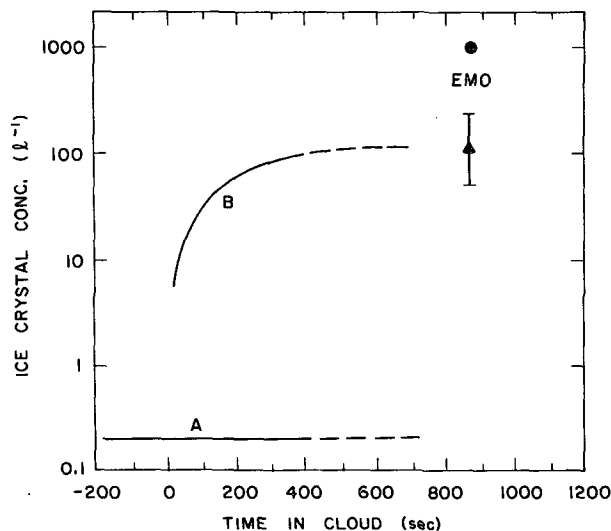


FIG. 15. Rates of formation of ice crystals for 10 January 1975. (Detailed explanations are given in the text.)

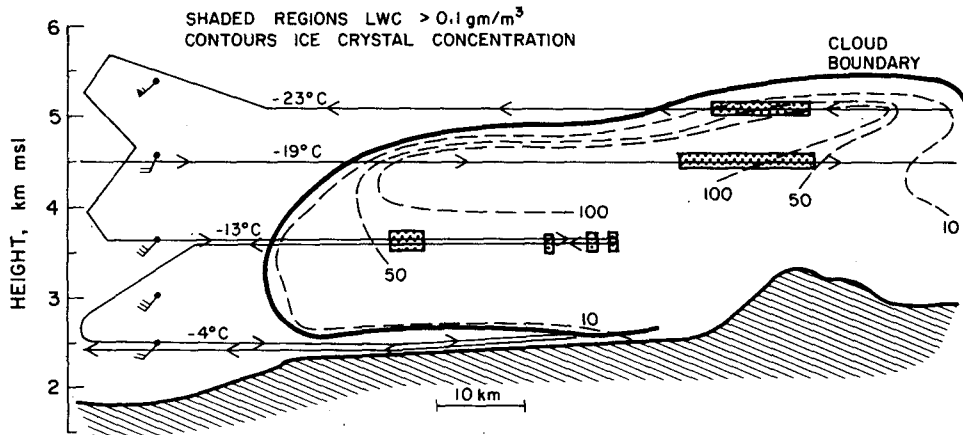
29 DEC 74
FLIGHT I

FIG. 16. Vertical cross section for the storm of 29 December 1974. The solid line with arrows shows the flight track, and the dashed lines are approximate contours of the ice crystal concentration (L^{-1}). The shaded regions indicate measured liquid water contents in excess of 0.1 g m^{-3} . Some representative temperatures are also given. The airflow was from the southwest, or from the left in the figure. Full wind barbs represent 5 m s^{-1} (after Cooper and Saunders, 1980).

what obscured in the downwind portions of the cloud where crystals fell from above into the lower parts of the cloud. The feature quite clearly apparent in the figure is that ice crystal concentrations rapidly increased to $50\text{--}100 \text{ L}^{-1}$ within about $1\text{--}2 \text{ km}$ of the upwind cloud edge at the -19°C and -23°C levels. Beyond that point, there was no additional increase in the ice crystal concentration. The sizes of the ice crystals increased with distance into the cloud so that $\sim 10 \text{ km}$ into the cloud there were few ice crystals smaller than $500 \mu\text{m}$. A region of low liquid water content was detected near the upwind edge of the cloud, but in this instance the crystal concentrations were so high and the updraft so gradual that the liquid water was rapidly depleted by the ice crystals. Except for this feature, the pattern of ice crystal development was very similar to that described in preceding sections for the Elk Mountain cap cloud cases; the deeper cloud here described, with its larger variation in temperature and greater length of parcel trajectories within the cloud, supports the generality of the pattern of ice crystal development observed in the cap clouds.

6. Discussion of ice crystal origins

In all three of the preceding case studies, most of the ice crystals apparently originated within $1\text{--}2 \text{ km}$ of the upwind cloud edge. The following paragraphs examine which possible mechanisms of ice crystal generation are consistent with those observations.

a. Ice multiplication

For secondary ice generation, or ice multiplication, it would be expected that crystal concentra-

tions would increase significantly beyond the cloud edge as the multiplication process continues. The absence of such increases in the clouds studied indicates that multiplication processes are not active in those clouds. More specifically, the Hallett and Mossop (1974) mechanism can be ruled out because in the situations we studied the droplets were not large enough, the temperature was too cold; and there were no riming objects near the upwind edges of the clouds. Similarly, splintering of freezing drops or crystal fragmentation can be ruled out because the conditions required for these processes were not present in the clouds under question. The rapid increase in ice concentration that occurs within a short distance of the upwind edge strongly suggests that a nucleation mechanism is responsible for the ice formation.

b. Deposition nucleation

The sharp increase in crystal concentration near the liquid water cloud boundary is not readily explainable on the basis of deposition nucleation, as the rate of deposition nucleation depends on ice and not on water supersaturation (Huffman, 1973) and shows no discontinuity when water saturation is reached. In the moderate updrafts of stratiform clouds, deposition nucleation should increase ice particles ahead of the liquid cloud edge, in ice-supersaturated regions, and should not exhibit a marked increase in activity as water saturation is reached. Thus, the major pattern, about two orders of magnitude increase in ice crystal concentration between points ahead and downwind of the edge of the liquid, cannot be explained by deposition nucleation.

The few crystals observed ahead of the clouds may have originated through deposition nucleation. (The flight data indicate that, in cap cloud cases, the gradually rising air reaches ice supersaturation several kilometers upwind of the visible cloud boundary.) The concentrations of these crystals are comparable to the results obtained by filter measurements of the deposition ice nucleus concentrations (Huffman, 1973).

c. Condensation-freezing nucleation

A nucleation sequence in which the same particle serves first as a condensation nucleus and subsequently as a freezing nucleus could produce the observed ice development near the cloud's leading edge, if it is postulated that only a small fraction of condensation nuclei would be capable of also initiating freezing. The condensation-freezing sequence is one for which there are no valid ice nucleus measurements, since to be realistic, such a measurement should have well-controlled supersaturation $< 1\%$, produced at a cold temperature. The absence of a marked increase in concentrations yielded when filter samples are processed above water saturation argues against this mechanism, although actual supersaturations achieved in such processing may be lower and more transient than those experienced in the clouds.

Experiments have been performed to detect freezing nuclei in the Elk Mountain cap clouds, by drop-freezing analysis of rime collected on a sampling rod (Vali, 1971), and by a melting and refreezing procedure similar to that of Hoffer and Braham (1962). Both kinds of tests revealed much lower concentrations of nuclei than would be needed to account for the observed ice crystal concentrations. Therefore, a corollary must be attached to the condensation-freezing nucleation hypothesis: freezing-nucleating ability is lost upon warming to temperatures $> 0^\circ\text{C}$, or is lost within relatively short times (on the order of minutes) for particles suspended in liquid water. The latter of these possibilities would also be consistent with the observed lack of further ice formation in clouds on additional cooling below the temperature of condensation.

d. Contact nucleation

Because the production of ice occurs only during a relatively short time (~ 100 – 200 s) a very rapid scavenging rate for the active contact nuclei would be required in order to give the observed development of ice crystals. Conventional estimates for scavenging times by Brownian motion (Slinn and Hales, 1971; Young, 1974) indicate that such scavenging rates would not be possible for any reasonable size contact nucleus. However, those estimates probably do not apply to the collection rates in these

clouds. Those estimates assume a steady-state collection rate applicable after the concentration of nuclei close to the cloud droplets is depleted and a concentration gradient is established about the droplet. In the case where the cloud droplets are freshly formed, the effective nucleus concentration near the drops is the ambient concentration. A gradient in nucleus concentration can only be achieved by scavenging, which would cause the droplet to freeze before the gradient could be established.

An estimate better suited to these clouds may be obtained by treating contact nuclei as a molecular species and calculating their collision rate (R_c) according to

$$R_c = 2r_d^2 \left(\frac{2\pi kT}{m} \right)^{1/2} nN,$$

where n is the number of contact nuclei per volume, m the mass of the contact nucleus, N the number of cloud droplets per unit volume, r_d the cloud droplet radius, k Boltzmann's constant and T the absolute temperature. This formula, which should give an upper bound to the rate of contact nucleus collection by Brownian motion, leads to a characteristic time for nucleus collection of

$$\tau = \frac{1}{2r_d^2 N} \left(\frac{m}{2\pi kT} \right)^{1/2}.$$

This characteristic time is considerably shorter than that corresponding to steady-state collection. With $N = 200 \text{ cm}^{-3}$ and $r_d = 4 \mu\text{m}$, τ is ~ 10 min for nuclei of $0.05 \mu\text{m}$ radius, and ~ 1 min for nuclei of $0.01 \mu\text{m}$ radius. Thus, contact nuclei of $< 0.01 \mu\text{m}$ radius would be required to account for the observed rate of development of ice crystals.

Some measurements of contact nuclei were made with a device in which aerosol particles are caused to contact supercooled water drops by means of electrostatic precipitation.⁶ Sampling of contact nuclei in Laramie, Wyoming, 100 km from Elk Mountain, yielded average concentrations of roughly 0.3 L^{-1} at -12°C , 1 L^{-1} at -16°C and 3 L^{-1} at -20°C . These contact-nucleus measurements represent the activity of particles $> 0.01 \mu\text{m}$ diameter; for smaller particles the collection efficiency of the instrument becomes very low.

The measured contact-nucleus concentrations are in fair agreement with ice crystal concentrations in the Elk Mountain clouds (Section 7c) although this may be fortuitous because of the difference in location for the two sets of measurements. In comparison with the San Juan clouds, the nucleus concentrations are an order of magnitude too low. Considering

⁶ Vali, G., 1976: Contact-freezing nucleation measured by the DFC instrument. *Third Int. Workshop Ice Nucleus Measurements*, Laramie, Int. Assoc. of Meteor. and Atmos. Phys., 159–178.

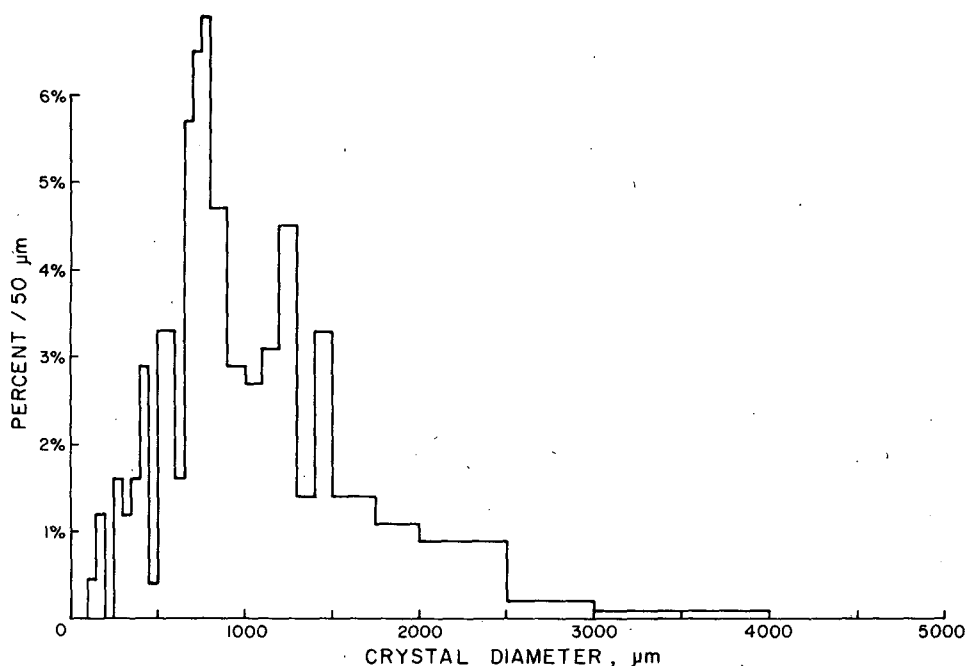


FIG. 17. Ice crystal size distribution from the flight of 17 March 1975 (0943 LT). The 2-D images were used to determine this size distribution.

the limitations of the contact-nucleus data and of the measurement technique itself, these discrepancies do not seriously weaken the plausibility of explaining ice development in the clouds by contact nucleation.

Thus, of the possible ice origins examined, the two that appear to be consistent with the observed pattern of ice evolution in clouds are condensation-freezing and contact nucleation. For each mechanism some properties have to be assumed for the nuclei which are at this time conjectural but which do not conflict with available evidence.

7. Supporting data

In this section, some interesting aspects of the wintertime clouds are presented and discussed in light of the ice crystal origins suggested in Section 6. Although these phenomena do not require the ice crystals to originate as suggested in Section 6, all are consistent with either of the postulated origins and therefore provide supporting evidence for them.

a. All-liquid cloud tops

It was observed in both stratiform and convective clouds that a thin layer at the tops of the clouds was often practically devoid of ice crystals. While the interiors of the clouds often contained ice crystal concentrations exceeding 10 L^{-1} , the thin upper cloud layer below the top usually had crystal concentrations $< 0.1 \text{ L}^{-1}$. This upper layer of typically 30 m depth had liquid water contents similar to the lower cloud, and the large droplet sizes indicated that the cloud there was not newly formed.

If most of the ice originates near the point of condensation, as suggested in Section 6, the ice-deficient region at the cloud top has a possible explanation: the ice simply falls from the liquid cloud region in which it formed. For a cloud which is ~ 5 min old, ice crystals should grow to sizes of $\sim 300 \mu\text{m}$, and such crystals should fall more than 30 m relative to the cloud parcel.

b. Ice crystal sizes

The sizes of ice crystals can be used to infer their ages, and hence, in situations of simple air parcel trajectories, their approximate regions of origin. This is possible because the growth rates of ice crystals are relatively well known as long as water saturated conditions are maintained, as is the case in the situations dealt with in this paper.

The common feature of the ice crystal size distributions found in cap clouds, and in San Juan storms of smooth airflow, is a well-defined mode and the absence of crystals much smaller than the mode. This pattern is most clearly evident in the clouds over the San Juan Mountains where longer crystal growth times are available. Fig. 17 shows an example of a size spectrum from a cloud over the San Juan Mountains, at a point where the estimated growth time of the crystals was 1000 s. The modal size of $\sim 800 \mu\text{m}$ is consistent with an origin near the cloud edge, as at -16°C the linear growth rate of crystals is $\sim 1 \mu\text{m s}^{-1}$. Only 10% of the crystals are $< 500 \mu\text{m}$ indicating that only $\sim 10\%$ of the crystals originated within 500 s of the observation

time. The larger sizes in the distribution represent aggregates of crystals.

c. Temperature trends

So far in this paper the emphasis was on the rate of generation of ice crystals with time. This characteristic could be documented for individual cases, so that no ensemble properties had to be assumed for the arguments. We now turn to a summary view of crystal concentration as a function of temperature for the two types of clouds discussed. The main purpose for this is to demonstrate that the postulated ice origin at the clouds' upwind edges yields a good correlation between concentration and temperature.

Temperature variations within individual cap clouds were $\leq 3^\circ\text{C}$, so the difference between the temperature at which the fully developed ice crystal concentrations were observed (near the mountain peak) and the temperature at the leading edge of the clouds was not great. This was not the case in the San Juan storms which were of greater depth and sometimes had more complex airflow structure. As a result, ice crystal concentrations in the San Juan storms did not correlate at all with the temperature of observation when data were included from all the clouds which were studied (Cooper and Saunders, 1980). However, selecting only those measurements which were taken in situations of smooth airflow

TABLE 1. Ranges of variables for the clouds sampled.

Atmospheric pressure	700–450 mb
Temperature of cloud formation	–9 to -23°C
Cloud droplet concentrations	200–600 cm^{-3}
Cloud liquid water contents	$< 1 \text{ g m}^{-3}$
Vertical velocities at condensation level	$< 3 \text{ m s}^{-1}$
CCN spectra (Elk Mountain)	$C = 326 \pm 127 \text{ cm}^{-3}$, $k = 0.57 \pm 0.4$

and within the upwind portions of the clouds resulted in the data shown in Fig. 18, where concentration is plotted against temperature of cloud formation (for the particular air parcel). Although the number of points is small, a correlation is evident. The trend line indicates a concentration of 20 L^{-1} at -16°C and an order of magnitude change in concentration for each 8°C in temperature.

In the same figure data are also shown for Elk Mountain cap clouds. The trend line for these data lies lower, 1 L^{-1} at -16°C , and is somewhat steeper than the line representing the San Juan data. This difference probably indicates a difference in ice nucleus populations.

8. Discussion

An important question to consider is the generality of the pattern of ice development, and of the postulated ice origins, which were described in the foregoing sections of this paper.

One aspect of this question is the range of some key variables in the clouds we studied. These ranges are approximately as given in Table 1. These characteristics can be summarized as those of wintertime stratiform clouds of midlatitudes, in continental, unpolluted, midtropospheric air.

Another aspect of the question is what other types of clouds have been found to exhibit the behavior described for the cap clouds and for the non-convective orographic storms. In our own investigations, we have found that wave-clouds (altocumulus lenticularis), and weak wintertime convective clouds (cumulus mediocris) fit the same pattern of ice development as the examples described in Section 6. The characteristics of these clouds still fit within the ranges given in Table 1. Measurements in wintertime upslope clouds show different features,⁷ but the results can be reconciled with an ice origin associated with cloud formation.

Comparisons with results from other studies are possible for the temperature dependence of ice crystal concentrations, and for inferences on ice origin which were drawn in some cases. In most papers,

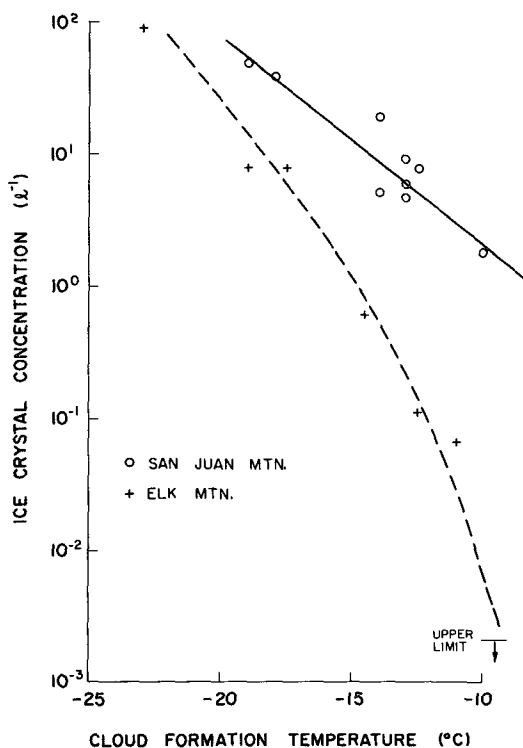


FIG. 18. Ice crystal concentration as a function of cloud formation temperature, for the measurements in the San Juan Mountains and for those near Elk Mountain.

⁷ Cooper, W. A., and G. Vali, 1976: Ice crystal concentrations in wintertime clouds. *Preprints Int. Conf. Cloud Physics*, Boulder, Amer. Meteor. Soc., 91–96.

TABLE 2. Comparison of observed ice particle concentrations.

Source	Temperature (°C)*			Ice particle concentration (L ⁻¹)**	Cloud type
	Cloud base	Point of observation	Cloud top		
Mossop (1972)		-9 to -10	-10 to -11	0.01-0.2	Sc (7 cases)
Jayaweera and Ohtake (1973)			-10	0.002-0.02	St
			-16	0.03-0.3	St
Hobbs and Atkinson (1976)			-10	0.03-500	Sc, St, As
			-16	20-1000	Sc, As
Heymsfield (1977)		-10		5-100	Ns (?)
		-16		5-100	
		-24		4-60	
San Juan storms (this paper)	-10†			2	Ns
	-16			20	
Elk Mountain (this paper)	-10†			<0.005	Ac
	-16			2	
	-24			200	

* Temperatures are given for either cloud base, observation point or cloud top, depending on the information supplied. Data are selected for temperatures of -10, -16 and -24°C, by interpolation if necessary.

** Where available, ranges are given which include ~90% of the observations.

† These temperatures are for the points of cloud formation, not cloud base in the strict sense.

insufficient detail is given on the distribution of ice crystals within the clouds to permit an evaluation of the time rate of appearance of ice, except for cases dominated by secondary ice production (Mossop, 1972; Hallett *et al.*, 1978) which are not useful to compare with the present results.

Reference has been made already in Section 2 to the conflicting published data on the agreement between ice crystal and ice nuclei concentrations in stratiform clouds. Table 2 recapitulates these data. It is evident from this table that only our data and those of Jayaweera and Ohtake (1973) show a clear temperature trend. Such a temperature trend is necessary and very likely sufficient evidence that nucleation (primary ice generation) is the source of the observed ice particles. This argument rests on the expectation that secondary processes in general have efficiencies which are not monotonic functions of temperature, as is the case with both the Hallett-Mossop mechanism and with the crystal-fragmentation mechanism.

Available data thus lead to the conclusion that there are important differences in the manner and rates of ice formation among the different stratiform clouds which have been studied. It can be surmised that these differences are due to regional differences in ice nucleus concentrations, and to differences in cloud parameters which might influence secondary ice generation. However, the possibility can not be ruled out that variations in observational procedures, and in interpretation, are responsible for some of the differences apparent in Table 2.

It is self-evident that the ice origin documented in this paper has no relevance to clouds, or cloud

parcels, which have condensation points at temperatures warmer than 0°C. Thus, convective clouds such as those described by Gagin (1975) and Dye *et al.* (1974), for example, can have ice origins similar to that described in this paper only to the extent that ice in those clouds formed in regions of mixing of cloud with cold ambient air in such a way that new cloud droplets were formed at temperatures < 0°C.

Acknowledgments. The authors are grateful for the excellent support of the Department's technical staff and pilots; and for the management of the project and facilities by Dr. D. L. Veal.

This research was sponsored by the Atmospheric Sciences Section, National Science Foundation, through Grants ATM 75-02515 and 77-17540, and through their support of the computer facility of the National Center for Atmospheric Research. Some flight data were also obtained under sponsorship of the Division of Atmospheric Water Resources Management, Bureau of Reclamation, U.S. Department of the Interior, under Contract 14-06-D-6801.

REFERENCES

- Auer, Jr., A. H., 1971: Observations of ice crystal nucleation by droplet freezing in natural clouds. *J. Atmos. Sci.*, **28**, 285-290.
- , 1972: Inferences about ice nucleation from ice crystal observations. *J. Atmos. Sci.*, **29**, 311-317.
- Cooper, W. A., and C. P. R. Saunders, 1980: Winter storms over the San Juan Mountains. Part II: Microphysical observations. *J. Appl. Meteor.*, **19**, 927-941.
- Dye, J. E., C. A. Knight, V. Toutenhoofd and T. Cannon, 1974: The mechanism of precipitation formation in northeastern Colorado cumulus. III. Coordinated microphysical and

- radar observations and summary. *J. Atmos. Sci.*, **31**, 2152–2159.
- Gagin, A., 1975: The ice phase in winter continental cumulus clouds. *J. Atmos. Sci.*, **32**, 1604–1614.
- Hallett, J., and S. C. Mossop, 1974: Production of secondary ice particles during the riming process. *Nature*, **249**, 26–28.
- , R. I. Sax, D. Lamb and A. S. Ramachandra Murty, 1978: Aircraft measurements of ice in Florida cumuli. *Quart. J. Roy. Meteor. Soc.*, **104**, 631–651.
- Heymsfield, A. J., 1977: Precipitation development in stratiform ice clouds: A microphysical and dynamic study. *J. Atmos. Sci.*, **34**, 367–381.
- Hobbs, P. V., and R. Farber, 1972: Fragmentation of ice crystals in clouds. *J. Rech. Atmos.*, **6**, 245–258.
- , and D. G. Atkinson, 1976: The concentrations of ice particles in orographic clouds and cyclonic storms over the Cascade Mountains. *J. Atmos. Sci.*, **33**, 1362–1374.
- Hoffer, T. E., and R. R. Braham, Jr., 1962: A laboratory study of atmospheric ice particles. *J. Atmos. Sci.*, **19**, 232–235.
- Huffman, P. J., 1973: Supersaturation spectra of AgI and natural nuclei. *J. Appl. Meteor.*, **12**, 1080–1082.
- Jayaweera, K. O. L. F., and T. Ohtake, 1973: Concentration of ice crystals in arctic stratus clouds. *J. Rech. Atmos.*, **7**, 199 p.
- Justo, J. E., and H. K. Weickmann, 1973: Types of snowfall. *Bull. Amer. Meteor. Soc.*, **54**, 1148–1162.
- Katz, U., and R. J. Pilie, 1974: An investigation of the relative importance of vapor deposition and contact nucleation in cloud seeding with AgI. *J. Appl. Meteor.*, **13**, 658–665.
- Kobayashi, T., 1961: The growth of snow crystals at low super-saturation. *Phil. Mag.*, **6**, 1363–1370.
- Mossop, S. C., 1972: The role of ice nucleus measurements in studies of ice particle formation in natural clouds. *J. Rech. Atmos.*, **6**, 377–389.
- Parungo, F. P., and H. K. Weickmann, 1973: Growth of ice droplets from frozen cloud droplets. *Beitr. Phys. Atmos.*, **46**, 289–309.
- Rogers, R. R., and G. Vali, 1978: Recent developments in meteorological physics. *Phys. Rep.*, **48**, 65–177.
- Rottner, D., and G. Vali, 1974: Snow crystal habit at small excesses of vapor density over ice saturation. *J. Atmos. Sci.*, **31**, 560–569.
- Ryan, B. F., R. R. Wishart and D. E. Shaw, 1976: The growth rates and densities of ice crystals between -3°C and -21°C . *J. Atmos. Sci.*, **33**, 842–850.
- Slinn, W. G. N., and J. M. Hales, 1971: A re-evaluation of the role of thermophoresis as a mechanism of in- and below-cloud scavenging. *J. Atmos. Sci.*, **28**, 1465–1471.
- Vali, G., 1971: Quantitative evaluation of experimental results on the heterogeneous freezing nucleation of supercooled liquids. *J. Atmos. Sci.*, **28**, 402–409.
- Vardiman, L., 1978: The generation of secondary ice particles in cloud crystal-crystal collisions. *J. Atmos. Sci.*, **35**, 2168–2180.
- Weickmann, H. K., 1972: Snow crystal forms and their relationship to snowstorms. *J. Rech. Atmos.*, **6**, 603–615.
- Young, K., 1974: The role of contact nucleation in ice phase initiation in clouds. *J. Atmos. Sci.*, **31**, 768–776.